Chapter

Laser-Matter Interaction in the Bulk of Semiconductor and Dielectric

Hong Liu and Chunlan Ma

Abstract

The research in the field of laser-induced materials processing is evolving continuously with new inventions in laser technology. This chapter mainly discusses the relevant physical mechanisms of laser ablation based on laser-matter interaction. Femtosecond laser excitation provides suitable conditions for studying the basic processes in irradiated materials, as compared to the duration of these processes, femtosecond laser pulses are sufficiently short. In the process of laser action on the matter, the thermal mechanism, charge carrier removal, thermal and structural effects, and other processes are extremely complex. The ultrashort laser pulse instantly puts the material in a strong nonequilibrium state characterized by hot electrons and cold ions. After the pulse ends, the electron transfers its energy to the ion through electron phonon coupling in sub-picoseconds. This heats up the phonon bath before the slow thermal effect can reconstruct the material. The electron effect plays an important and possibly dominant role in the laser ablation of nonmetallic solid surfaces. This review first describes the mechanism of laser-matter interaction from the perspective of energy, summarizes the electronic excitation and energy relaxation paths of light on semiconductors and dielectric materials, focuses on the electronic excitation and relaxation mechanisms in laser-induced ionization, desorption, and ablation, and finally analyzes the above-mentioned related processes from the perspective of material structure relaxation.

Keywords: laser-matter interaction, ionization, desorption, ablation, electronic excitation, energy relaxation

1. Introduction

Laser ablation (i.e., laser machining (LM)) as a noncontact, wear-free machining process is a promising method to machine difficult-to-cut materials, such as silicon nitride, silicon carbide, aluminum oxide, and boron nitride.

Surface ablation based on high power ultrashort pulse laser plays an increasingly important role in material processing and device preparation technology [1–3]. Classically, the interaction between laser and matter is described by the Beer Lambert law, which states that the transmittance of monochromatic light passing through a material

sample decreases exponentially with the length of the optical path, regardless of the incident intensity. This corresponds to a linear light absorption process, as is commonly assumed for nanosecond laser pulses [4]. Electronic defects are generated by initial laser irradiation, changes in absorption characteristics, and laser energy deposition of photons in the middle and later stages of a given or subsequent laser pulse. The ablation plume generated by laser action effectively shields the sample from the influence of laser [5–8], and the plume can keep transparent to the laser at low flux because any free electrons will recombine with ions before being accelerated to ionization energy, which is easy to be absorbed by free electrons in the plume so that they can quickly heat and then ionize the current neutral substance. When the ionization rate exceeds the recombination rate of free electrons and ions, the number of ionized neutral substances doubles. Laser plasma interactions are no longer characterized by classical light absorption, as various nonlinear effects, such as direct collision and field-induced ionization and dissociation reactions, as well as reverse bremsstrahlung [4, 8–10] have emerged. The plume can be transparent to the laser at low flux because any free electron will recombine with the ion before being accelerated to ionization energy. Scholars have established dual temperature models and multi-plasma coupling models for the physical mechanisms of the interaction between laser and matter mentioned above. But there are still many controversies. The above processes can lead to photothermal effects (injection, ionization, vibration heating, melt discharge, evaporation, and plasma formation) and photochemical (bond breaking and generation of new components) processes, which are used for various laser processing and coherent structure preparation [11].

Based on the electronic process of nanosecond and shorter pulse laser ablation in pure semiconductors and dielectric materials, this chapter constructs the dynamics and dynamics images of laser-induced desorption and ablation of nonmetallic crystal surface, expounds the physical mechanism of laser solid interaction, and then gives the physical process that causes the change of bonding state, particle emission, and final ablation. After providing the ionization, desorption, and ablation mechanisms of laser on dielectric and semiconductor surfaces, we construct ionization, desorption, and ablation models under the irradiation limit of strong and weak laser pulses on solid materials, and qualitatively analyze the dynamic mechanism of material structure relaxation under the action of pulsed laser. Finally, a brief summary of the content of this chapter was provided.

2. The physical mechanism of the laser-matter interaction on the different pulsed laser intensity (low and high)

2.1 Basic principle of laser-matter interaction

Bill Lambert's law gives a macroscopic description of the interaction between laser and material and points out that the transmittance of monochromatic light passing through the material sample decreases exponentially with the length of the optical path, and is independent of the incident intensity, which is a linear optical absorption process [4]. However, in the high flux region at a sufficiently long wavelength, this approximation becomes ineffective, where the ablation plume formed effectively protects the sample from the laser [5–7].

The absorption mechanism of laser varies greatly among different materials. For metal nanoparticles, optical absorption is attributed to the collective oscillation of

conduction band electrons in the laser field [12–15]. Due to the transient net charge on the particle surface during the oscillation process, a surface plasma is formed. The surface plasmon absorption band depends on the size and shape of the nanostructure (see **Figure 1**) [12, 14–16]. Irregular nanostructures, such as nanocubes and nanoprisms, can generate wider peaks over a wide wavelength range [13, 15, 16]. For heavily doped semiconductors, optical absorption is based on a similar principle of conduction band electron oscillation, while additional absorption is formed due to the excitation of optical phonons, interband transitions, and the dielectric background of polarization generated by all high-frequency excited tails in the material [17]. For pure semiconductors and dielectric materials, the interaction process between pulsed laser and materials is as follows. When irradiated by low-intensity and long-wavelength lasers, the material has little absorption of laser radiation, which will not be discussed here. If the intensity of the incident laser reaches the ablation threshold or the ultra-short wavelength laser acts on the material so that the material can absorb enough energy, the laser will damage the material. Research shows that the production of high-density plasma is the main reason for the damage of high-purity semiconductor and electrolyte materials. The ultrashort pulse laser causes the plasma structure of extremely high density ($10^{18} - 10^{20} cm^{-3}$) free electrons in the dielectric material, simultaneously accompanied by a large number of ionization phenomena.

2.2 Influence of pulse laser parameters on laser-matter interaction

Laser wavelength(λ), the average pulse laser intensity (I_L) [18] and pulse duration (t_{pulse}) are several main parameters that affect the interaction mechanism between laser and material. For lasers with different pulse durations, the mechanisms leading to energy absorption and target ablation are completely different (**Figure 2**). Research shows that if the duration of the laser pulse on the metal workpiece is shorter, the quality of laser ablation will be improved [20, 21].

Thermal diffusion and direct interaction between laser and material can ablate the material. Due to the fact that thermal energy can diffuse in any direction of the material, related erosion can also occur in any direction. Laser ablation is mainly based

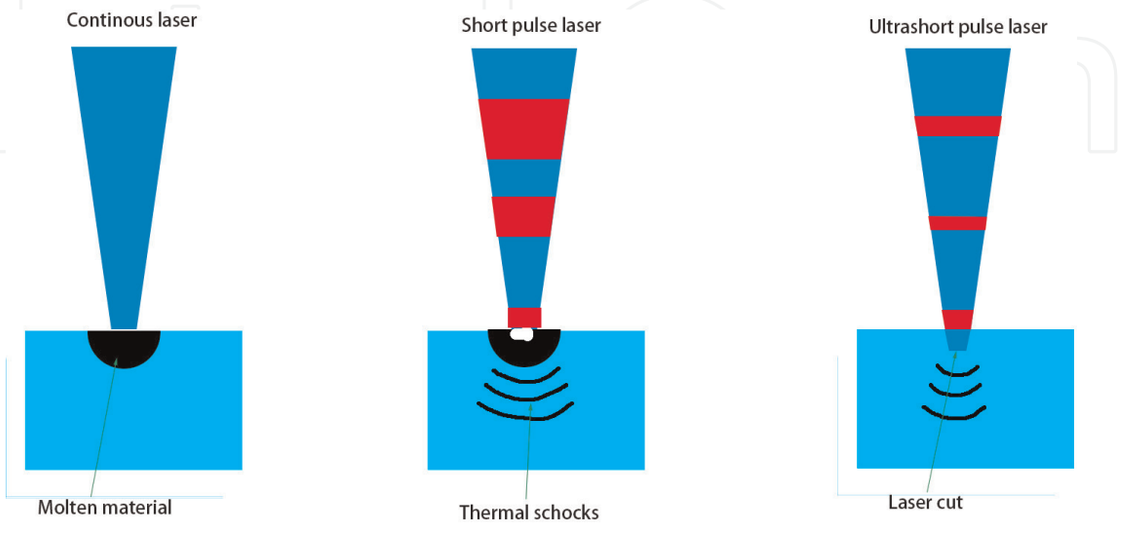

Figure 1.
Laser-material interaction in continuous, short pulse (nanosecond) and ultrashort pulse laser. Reproduced from ref. [19].

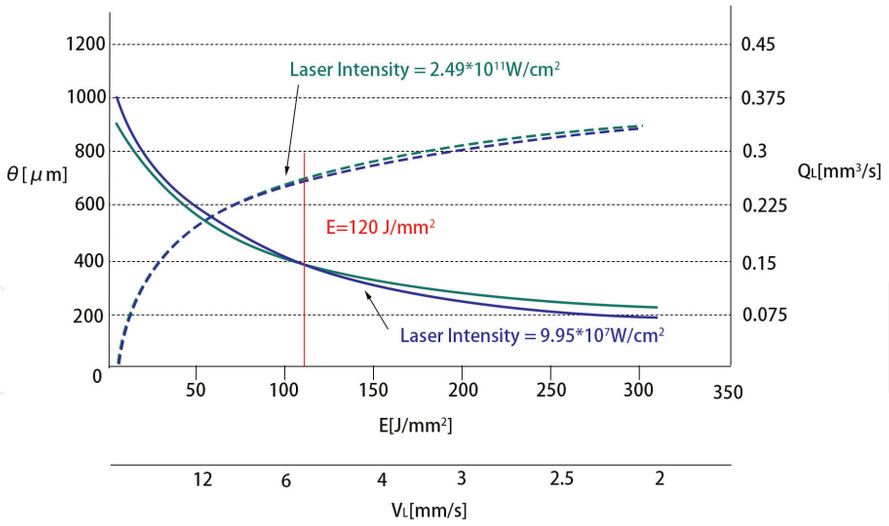

Figure 2.
Effect of laser input energy density per material removal rate. a_{e-L} *vs.* $E_{L-input}$ *and* Q_L *vs.* $E_{L-input}$. *Reproduced from ref. [19].*

on the direct interaction between the laser beam and the surface rather than the thermal diffusion in the material volume. Therefore, material ablation is mainly conducted in the direction of laser radiation. The energy distribution of the laser beam satisfies the Gaussian distribution model, with approximately 90% of the laser beam energy concentrated at the center of the laser beam (in spots with radii less than 30% of the laser spot radius) [22]. Reduce laser input energy density $E_{L-input}$ by increasing laser scanning speed can modulate the laser cutting depth at the cutting center, rather than the boundary of the irradiation area, to form a V-shaped laser cutting. In addition, laser ablation depth a_{e-L} for laser input energy density $E_{L-input}$ changes in a sensitive response compared to other cutting sizes. The correlation between laser input energy density $E_{L-input}$, laser ablation depth a_{e-L} and material removal rate Q'_L is shown in **Figure 3**. The relevant analytical relationship is shown in Eq. (1):

$$a_{e-L} = Bln\left(\frac{E_{L-input}}{A}\right) \tag{1}$$

In Eq. (1), A and B are constant values. Due to ablation depth a_{e-L} should always be zero or positive, the minimum value of laser input energy density $E_{L-input}$ should be equal to a. If $E_{L-input} = A$, then $a_{e-L} = 0.0$ μm. The values of A and B vary with the average pulse intensity I_L changes.

Eq. (1) is similar to the blow-off model for laser ablation, which assumes that exceeding characteristic threshold laser energy causes the ablation process. In this model, depth of ablation is given by the following equation [23]:

$$a_{e-L} = \gamma ln\left(\frac{E_{L-input}}{E_{th}}\right) \tag{2}$$

a_{e-L}: Laser ablation depth
E_{th}: Laser energy threshold
γ: Constant value.

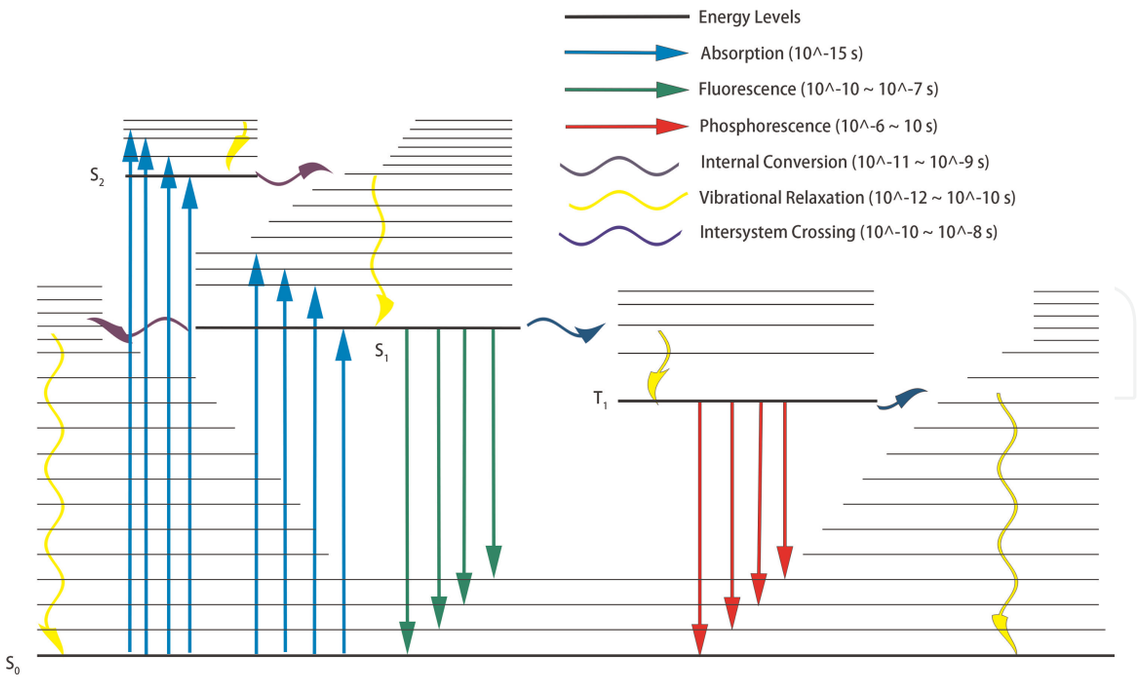

Figure 3.
Typical Jablonski diagram shows possible radiative and nonradiative transitions S_0 is the singlet ground state of the molecule, S_1 is the first excited singlet, S_n is the nth excited singlet, T_1 is the first excited triplet, and T_n the nth excited triplet.

The constants A and B in Eq. (1) depend on the inherent characteristics of the laser (such as wavelength λ and I_L) and material characteristics. In the blowing model, the decrease in I_L leads to the increase in threshold laser energy E_{th} and laser ablation depth and the decrease in ablation efficiency of each laser pulse [24]. The efficiency of laser ablation can be quantified by the process parameters, such as the specific ablation energy (e_L), as the laser energy required to ablate a unit volume of material. The lower the specific ablation energy e_L, the higher the laser ablation efficiency.

Based on nanosecond laser ablation, the interaction between laser and material is based on the thermal mechanism. From a thermodynamic perspective, material erosion is mainly due to the melting and evaporation of the irradiated material. The key ablation factor in the thermal process is the material's gasification process. During this process, if the energy absorbed by the molten or solid material is insufficient to evaporate, it only leads to heating and thermal damage to the irradiated surface. The consumption of laser energy in deep laser cutting leads to the decrease of I_L and results in an increase in material melting and thermal damage, rather than material evaporation.

Above, we have made a qualitative analysis and description of the interaction between laser and matter from the energy perspective. The underlying physical mechanism of laser-material interaction will be described and analyzed in the following sections.

3. Interaction of photons with semiconductor and dielectric

The mechanism that laser acts on the surface of semiconductor or dielectric materials to cause changes in the electronic state inside the materials can be explained by Jablonski diagram.

Figure 1 is a typical Jablonski diagram of the evolution process of state change and energy transfer of materials after light irradiation.

In the Jablonski diagram, several different pathways show how electrons receive and then dissipate the energy of photons from specific wavelengths. Therefore, most graphs begin with the electronic state of the ground state and then return to the ground state. The initial energy comes from the absorption of light interacting with matter, that is, the blue straight arrow in the figure. The absorbed energy will cause electrons to transition from the ground state to the excited state of a higher energy level. We focus on the physical connotation of absorption, vibrational relaxation and internal conversion, intersystem crossing, and timescale. The specific descriptions of the above cases are as follows:

3.1 Absorption

Absorption belongs to radiation transition because in this process, the molecule absorbs photons before it transitions from the lower electron level to the higher electron level. The energy of photons is converted into the internal energy of molecules. Absorption is the fastest transition in the Jablonski diagram, which occurs on the timescale of femtoseconds. At room temperature, based on the Boltzmann distribution, most molecules in the group will be in the lowest vibrational energy level of the ground state, and the absorption of photons will raise the molecule from S_0 to one of the vibrational energy levels of the single excited state $(S_1, S_2, \ldots)$. Restricted by the conservation of angular momentum, the molecule cannot be directly excited to the triplet state excited state $(T_1, T_2, \ldots)$.

3.2 Vibration relaxation and internal conversion

After being excited, electrons cannot be stably maintained in the excited state, but tend to return to the more stable ground state, which must be accompanied by energy dissipation. The first is through vibrational relaxation, a nonradiative process. This is represented on the Jablonski diagram as a curved arrow between the vibration levels. Vibrational relaxation is when the energy transferred from photons to electrons is fed into other vibrational energy levels as kinetic energy. This kinetic energy may remain in the same molecule or may be transferred to other molecules around the excited molecule. This process is also very fast, between and picoseconds. Since this is a very fast transition, and this relaxation occurs between the vibrational energy levels, usually electrons do not change from one electron level to another by this method.

However, if the vibrational energy level and the electronic energy level overlap severely, the excited electrons may transition from the vibrational energy level in one electronic state to another vibrational energy level in a lower electronic state. This process is called internal conversion and is similar in mechanism to vibrational relaxation. It is also represented on the Jablonski diagram as a curve between two vibration levels in different electronic states. The internal conversion occurs due to the overlap of the vibrational energy level and the electronic energy level state. This overlap increases the probability of electron transition between vibrational levels, which will reduce the electron energy level. Therefore, internal conversion and vibrational relaxation occur in the same time range, which is a way for molecules to dissipate energy from light excitation. However, due to the lack of vibration and the overlap of electronic energy states and the large energy difference between the ground state and the first excited state, the internal conversion of electrons back to the ground state is

very slow. This slow return to the ground state causes other transfer processes to compete with the internal conversion in the first excited state. Both vibrational relaxation and internal conversion occur in most excitations, but rarely in the final conversion.

3.3 Intersystem crossing

Another way for molecules to absorb energy is through cross-mediation between systems. Based on the characteristics of electron spin multiplicity, we can relax from the excited singlet state to the excited triplet state. This is the slowest state transition process in the Jablonski diagram, several orders of magnitude slower than fluorescence. According to the transition selection rule, this slow transition was originally a prohibited transition. Based on the coupling of vibration factors and selection rules, transitions become weaker and can compete with the timescale of fluorescence. The crossover between systems results in different paths for returning the ground state electronic state. The direct transition is phosphorescence, which corresponds to the radiative transition from the excited triplet state to the singlet ground state. This is also a very slow and prohibited transition. Another possibility is to delay fluorescence and return to the first excited singlet state, causing the emission to change to the ground state electronic state.

Most molecules go from the excited state to the ground state through other nonradiative transition paths, so they do not exhibit fluorescence or phosphorescence behavior. On the one hand, they can transfer energy between molecules through molecular collisions or external transformations. On the other hand, energy is transferred between molecules through quenching, based on the overlap of absorption and fluorescence spectra. These pathways are all nonradiative processes, and when molecules relax to the ground state, they compete with fluorescence processes.

3.4 Timescale

The Jablonski diagram shows the types of transitions that may occur in specific molecules. The probability of each transition occurring depends on the timescale of the corresponding process, and the faster the process, the greater the probability of occurrence, based on the selection rules and their relaxation. **Table 1** lists the average timescales of basic radiative and nonradiative processes.

Transition	Timescale	Radiative process?
Internal Conversion	10^{-11}–10^{-9} s	No
Vibrational Relaxation	10^{-12}–10^{-10}s	No
Absorption	10^{-15} s	Yes
Phosphorescence	10^{-6}–10 s	Yes
Intersystem Crossing	10^{-10}–10^{-8} s	No
Fluorescence	10^{-10}–10^{-7} s	Yes

Table 1.
Average timescales for radiative and nonradiative processes.

It can be seen from the data in **Table 1** that almost all nonradiative energy transfer of excited electrons is completed in the nanosecond time range. This is the basis for the subsequent analysis of laser-material interaction.

4. Electronic mechanisms of semiconductor and insulator in ionization, desorption, and ablation induced by laser

4.1 Absorption and energy relaxation

In semiconductors and insulators, electron-hole pairs generated by photon absorption relax, forming localized and excited electron and vibration states. The electronic energy absorbed by photons is converted into nuclear motion and finally into desorption, which depends on the characteristics of the electron-lattice interaction. Of course, not all electron excitations lead to desorption. The electron-hole pair may lose energy or radiation recombination and be lost in the precursor channel for desorption. Various excitation and relaxation paths from the main photon solid interaction to the relaxation excited state are schematically shown in **Figure 1**.

The mass transfer and ionization mechanisms induced by laser can be roughly divided into thermal and nonthermal mechanisms. Thermal mechanisms include normal evaporation, photomechanical spalling, and phase explosion, while nonthermal mechanisms include electron transition-induced desorption, electrostatic ablation, Coulomb explosion, and so on. The peak power, tunable wavelength, continuous wave (CW), pulse duration, and precise beam optics of the laser beam provide micro/nano level controllable processing.

When a sufficiently strong laser pulse irradiates the material surface, the material undergoes different stages. These phases can be classified according to their duration. For example, chemical reactions occur on the femtosecond timescale (phonon vibration period). Similarly, electron motion is the key to any material modification, and it occurs on the timescale of attoseconds (the electrons need about 150 times per revolution of the atomic nucleus) [25]. This section explains these ultrafast mechanisms of electron state evolution and electron-lattice interaction in the nanosecond and femtosecond ranges. Furthermore, the desorption and ablation mechanism of the material under the action of a pulsed laser is explained.

The process of laser action on the material surface sequentially involves absorbing pulse energy, distributing energy to electronic subsystems, and then relaxing based on electron-phonon interactions [26, 27]. The absorption and distribution of energy occur within the femtosecond duration, while the electron-phonon interaction occurs within the picosecond duration. Such a nanosecond pulse interacts with matter, and all three processes will be completed within the duration of the pulse. The nanosecond pulse energy is used as a continuous energy source for the above three processes. When a laser with photon energy greater than Fermi energy is absorbed by the surface of the material, it directly leads to the excitation of electron transitions. The excited atoms relax through the combination of electron-phonon interaction, radiation recombination, Auger recombination, and carrier diffusion. According to the intensity of the laser pulse, the distribution is based on two different paths of heating and ablation, leading to melting. The excitation mechanism of ultrashort laser pulses causes the material to be in a strong nonequilibrium state characterized by hot electrons and cold ions. After the pulse ends, the electron transfers its energy to the ion through electron-phonon coupling in sub-picoseconds. This heats up the phonon bath before the slow thermal effect

can reconstruct the material [18, 28–30]. In metals, electrons and phonons will reach the same temperature in this way, allowing for any subsequent thermal phase transition when the system is in internal equilibrium. In semiconductors and insulators, the generated excitons undergo additional recombination through radiative or nonradiative recombination, where the latter implies exchange with phonons [31]. Due to the presence of surface states and the formation of net charges after electron emission, the material surface needs to be regarded as an independent region with its own excitation and thermal mechanism. In other words, on the timescale equivalent to the relaxation time of the quasiparticle and the length scale similar to the average free path of quasiparticle, the quasiparticle pass through the structure unimpeded and mainly scatter at the interface. For example, in macroscopic objects, heat and phonon transport exhibit diffusion over a long period of time, but when the length and timescales become narrower, their properties become ballistic. The average free path of phonons can be as large as 300 nm but decreases with increasing temperature [31, 32].

In the case of femtosecond laser, a sufficiently strong laser pulse can generate free carrier density in the conduction band as high as 10^{20} to $10^{22}/cm^3$ [29, 33]. The high-density free charge carriers result in mutual shielding in the conduction band and heating before the relaxation of electron-phonon interactions. The time delay caused by free carrier shielding in the conduction band leads to bond weakening, causing band gap collapse, and leading to the transition from semiconductor to metal.

In addition, the electron-phonon relaxation process in femtosecond mode occurs after the pulse, and the duration of the femtosecond pulse is sufficient to cause the initial absorption part of the laser pulse energy to generate plasma on the material surface. The plasma absorbs the remaining part of the incident pulse through the reverse bremsstrahlung process (**Figure 4**). The absorbed pulse energy of the plasma accumulates deep in the material, resulting in a higher-density plasma [35].

4.2 Ionization mechanism

Multiple excitation mechanisms are used to explain the interaction between laser and condensed phases. Research has clearly pointed out the importance of laser and sample characteristics, as there is no universal mechanism to explain every situation. Starting from sufficiently high laser intensity for ablation or breakdown, the duration of the pulse determines whether thermal and hydrodynamic effects occur during the

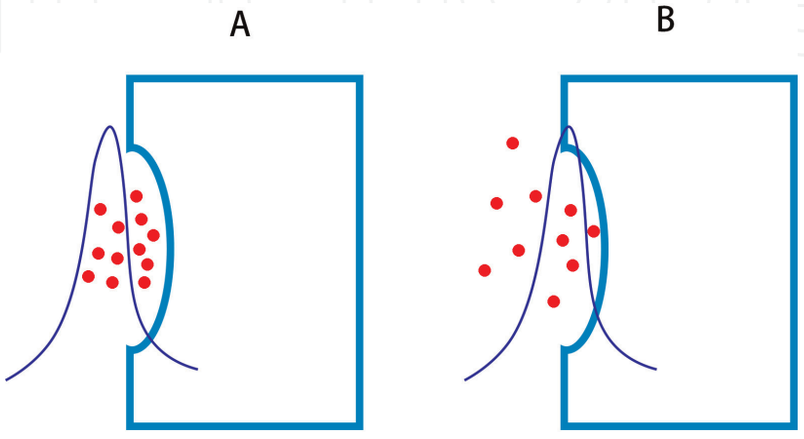

Figure 4.
Pulse propagation, (A) plasma generation, and (B) plasma expansion and absorption in femtosecond regime. Reproduced from ref. [34].

radiation period. For femtosecond pulses, this process can only begin after the irradiation is terminated. During nanosecond pulses, it is usually assumed that there is a balance between excitation and relaxation processes to maintain the material in an overall electrically unexcited state, and the energy of the transient excited electrons is rapidly transferred to the heavy species. This allows a purely thermal description using classical hydraulics and thermodynamics [6]. In the initial stage of laser interaction, nonthermal processes may have significant contributions that cannot be ignored. The wavelength of the laser further determines the properties of the excitation process. Ultraviolet radiation can usually cause electron excitation or ionization events using a single photon. In nonmetallic solids and liquids, ionization in this case corresponds to the transition of valence electron to the conduction band in the Jablonski diagram [36–39]. For a single photon with a longer wavelength, excitation and ionization can be realized through the nonlinear effect caused by high laser irradiance. Strong photon flow can be taken as a collective, and valence electron can be excited by field-induced ionization. Based on wave-particle duality, this mechanism can be distinguished as a function of multiphoton, tunneling, and barrier excitation intensity [40]. For example, multiphoton absorption enables infrared lasers to directly boost electrons within an energy range exceeding one of the constituent photons. Only when the ionization rate of the tunnel is fast enough relative to the frequency of light can quantum tunneling be achieved at higher irradiance [40]. From the moment of producing quasi-free electrons, excitation, and ionization can further occur through charge carrier acceleration and collision, as well as reverse bremsstrahlung radiation [4, 40]. Direct impact ionization should not be the main mechanism in dielectric materials. The above excitation mechanism can serve as a source for understanding the voltage-induced breakdown mechanism of condensed materials.

The dielectric surface is converted into plasma by ultrashort pulses of about 100 fs with an average intensity of about $1 \sim 10 TW/cm^2$ [41, 42]. It is conventionally suggested that the ionization threshold is achieved when the electron number density in the conduction band reaches the critical density $n_c = m_e\omega^2/4\pi e^2$, corresponding to the incident laser wavelength [43]:

$$n_c = \int_0^{t_{ion}} W(I(r,z,t))dt \tag{3}$$

where $W\ (I\ (r,z,t))$ is the sum of ionization rates generated by electron collisions and multiphoton mechanisms, respectively. The ionization time is represented by the time required to reach the critical density. Therefore, the breakdown threshold depends on the injection amount. The degree of impact of collision and multiphoton ionization on the ionization rate depends on the oscillation energy of electrons in the laser field., $\varepsilon_{osc} = e^2E^2/4m_e\omega^2$ (averaged over the light period and for linear polarization), and the ionization potential, J_i, or band gap Δ_g [44]. The ratio of ionization potential (or band gap) to the energy of oscillations is the adiabaticity parameter, $\gamma = \Delta_g/\varepsilon_{osc}$. It can be used to separate different ionization states. When $\gamma > 1$, multiphoton ionization is dominant. Electron collision ionization is the main ionization mechanism in the long pulse region.

4.3 Desorption and ablation

The excitation and thermal processes in laser-irradiated materials lead to the rapid heating of phonon baths. For femtosecond laser pulses, rapid energy deposition leads

to so-called inertial stress limitation [45, 46], which is due to the accumulation of strong compressive stress and the inability of materials to expand in such a short time. The subsequent relaxation of these stresses creates underground voids, leading to liquid surface layer separation and droplet ejection [45]. Therefore, during the ultrafast laser pulse, heat conduction and hydrodynamic movement are still limited, thereby reducing the thermal damage and heat-affected zone on the target [47]. There may be two explosion states, from the photomechanical spallation at lower flux to the phase explosion at higher flux [45]. Strong recoil pressures of up to 1*GPa* have also been reported for longer or continuous pulses [48], but the shielding of the laser beam by the jet plume can play a role, especially at longer wavelengths. This significantly reduces ablation efficiency compared to femtosecond pulses [49, 50]. However, for nanosecond pulses with shorter wavelengths, the ablation efficiency is still very high, and the inverse bremsstrahlung in the laser plume interaction can be ignored [4].

In this section, it is worth noting that three studies of Russo's group, one of which studied the particle size and shape [50], and two of which focused on the delayed particle emission effect [51, 52]. It was found that femtosecond pulses on brass produced particles with a diameter of about 100 nm, forming large aggregates, while nanosecond pulses produced spherical entities ranging from hundreds of nanometers to thousands of nanometers [50]. According to two other studies, a laser pulse on silicon with a duration of 3 ns first removes mass by normal evaporation during the pulse period and then sprays micron-sized particles due to delayed explosive boiling after 300 to 400 ns [51, 52]. This delay can be explained by the nucleation and growth delay of bubbles in the superheated melt. Note that this mechanism can also be effective for femtosecond pulses. Compared with nanosecond laser ablation, the limited heating of the material around the melt in the femtosecond case may even lead to no convex edge above the surface [53].

There are still many questions about the origin of molecular species in the ablation plume, because they may be by-products of evaporation or photomechanical spallation, or phase explosion, released directly from the sample surface or from ejected nanoparticles or droplets. In the case of femtosecond pulses, the generation of molecular fragments is high over a wide wavelength and flux range [7] and also depends on the position of the laser focus relative to the sample surface [54]. Nanosecond pulses are not suitable for maintaining molecular structure at infrared and ultraviolet wavelengths. For infrared, this is due to plasma heating caused by the interaction between low molecular generation rate at low flux and laser plumes at high flux [7]. Nanosecond ultraviolet pulses do not have this shielding effect and will destroy molecular bonds based on high photon energy and strong thermal effects. Two more controversial mass transfer mechanisms in laser ablation are electrostatic ablation and Coulomb explosion. Both assume that ions are directly released from the sample surface into the gas phase through a strong field effect. As a first step, the laser generates a positively charged surface layer through a sufficiently short wavelength photoelectric effect or field-assisted thermionic emission. According to the electrostatic ablation mechanism, surface ions are then pulled into the gas phase by the electric field induced by the emitted electrons [55, 56]. However, the Coulomb explosion is caused by the repulsive force between positive ions in the surface layer [55, 56]. The process occurs ultrafast, which explains the early ion emission during femtosecond pulse ablation (see **Figure 5**). This mechanism is also controversial, as it is believed that surface charges are quickly eliminated through charge compensation through the redistribution of conductive electrons within the body.

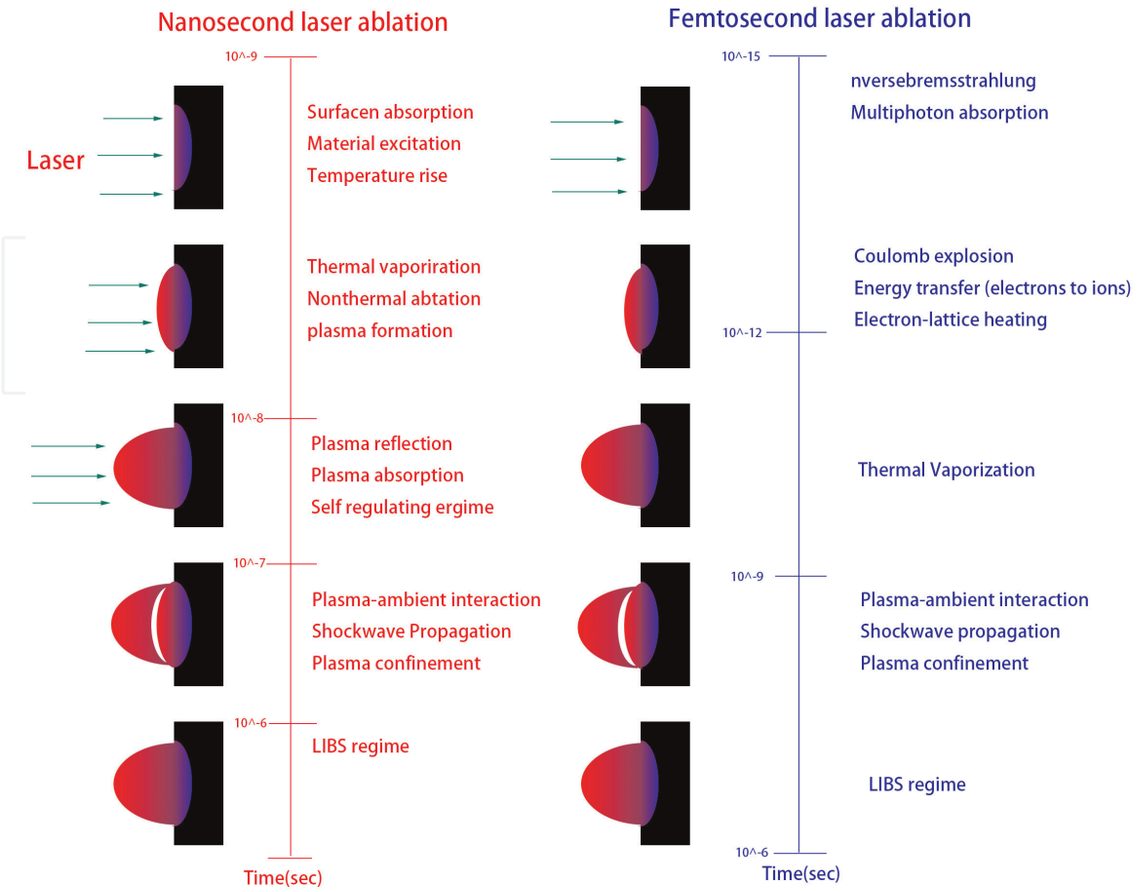

Figure 5.
Timescales of various processes taking place during and after the laser pulse in (left) nanosecond and (right) femtosecond laser ablation. Reproduced from ref. [4].

5. Electron-lattice interactions and material structural relaxation

5.1 Relaxation of a nonequilibrium phonon distribution induced by laser irradiation

Laser action on a substance first excites electrons, which transmit the stimulated energy to the nucleus and convert it into driving energy for nuclear motion, causing atoms, ions, and molecules to eject from the material surface, forming laser-induced desorption and ablation. Based on a series of electron lattice interactions, such as phonon scattering of free electrons, phonon emission, local lattice rearrangement, and configuration changes, and the rate and dynamic characteristics of transformation, are influenced. The configuration changes caused by the self-trapping of holes and excitons, defect formation and reaction, and electrical interactions between defects and lattice ions lead to surface decomposition.

Femtosecond laser excitation provides a suitable condition for studying the basic process in irradiated materials, because the duration of laser pulse is much shorter than the time required for the energy transfer process in the excited materials. **Figure 6** shows a comparison of thermal mechanisms, charge carrier removal, thermal effects, and structural effects. According to the ultrashort laser pulse excitation mechanism described in Section 4, laser radiation forms strong nonequilibrium states characterized by hot electrons and cold ions in the material. At the end of the pulse,

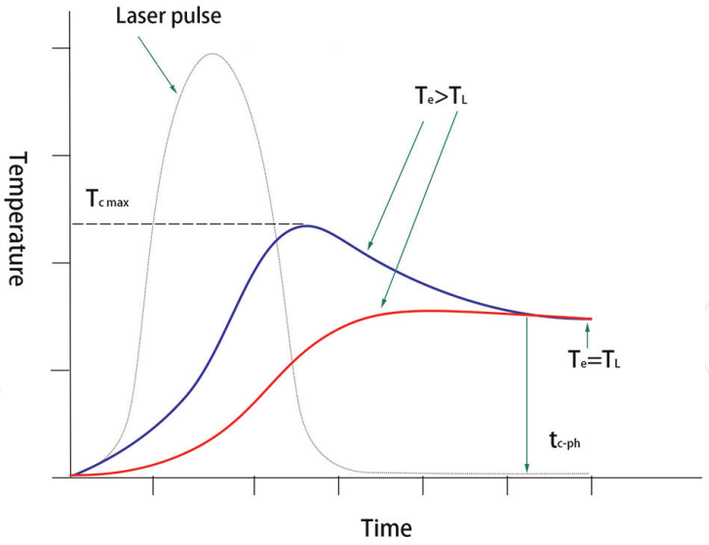

Figure 6.
Qualitative time dependence of electron and lattice temperature in the skin layer. The dotted line is a Gaussian shape of fs-laser pulse; t_{e-ph} indicates the energy equilibration time. Reproduced from ref. [56].

energy is transferred to the ion within sub-picoseconds through electron-phonon coupling. In semiconductors and insulators, excitons are generated simultaneously, and they will undergo radiative or nonradiative recombination, which involves exchanging energy with phonons. However, the simulation of silicon shows that the phonon system is in a nonequilibrium state within several hundred picoseconds [57]. Therefore, this nonequilibrium may affect the early stage of the thermal effect. In this regard, it seems to be more recommended to consider from the nonthermal and thermal timescales than from the nonthermal and thermal processes.

5.2 Dynamic mechanism of atomic site change in materials under the action of pulsed laser

In the initial stage of laser interaction with semiconductors and insulators, heated electrons are rapidly excited, and atoms vibrate almost undisturbed near their equilibrium positions. When the laser pulse ends, the electron reaches its maximum temperature and produces an electron temperature gradient in the surface layer, which generates a driving force on the surface layer. This force is proportional to the electron temperature gradient and acts on atoms, causing coherent motion of the atoms. This force is generated at a time shorter than the phonon period ($t_{ph} = 2\pi/\omega_{ph} \sim$few hundred fs) and produce rapid atomic shifts. The magnitude of this force is proportional to the absorbed energy density. The elastic force that causes atomic vibration in an undisturbed solid is also greater than the electric force at the energy density of the melting equilibrium enthalpy. The electric force only acts as a short pulse, triggering atomic vibration at the "cold" phonon frequency. From a time perspective, the next stage of atomic vibration corresponds to harmonic vibrations with "cold" phonon frequencies, which persist during the energy transfer from electrons to the lattice until the lattice reaches a temperature close to the melting point. Afterward, atomic vibrations gradually lose their harmonic characteristics, and nonlinear interactions between different phonon modes will dominate, ultimately transforming the solid into different phases or disordered states.

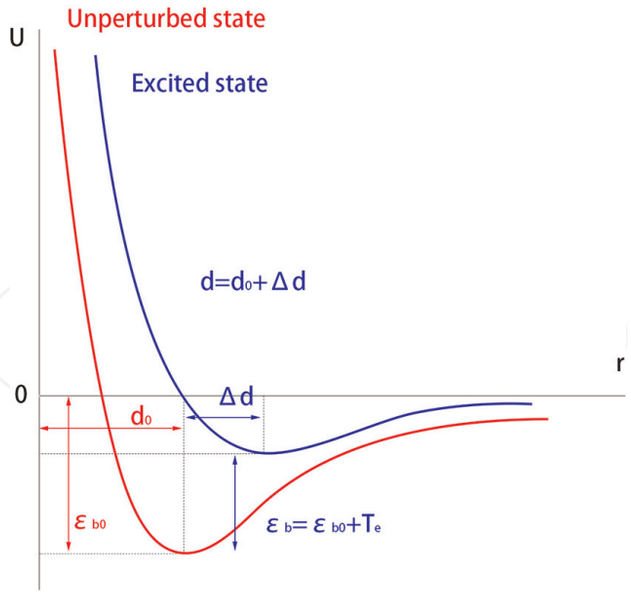

Figure 7.
Qualitative picture for the change of the potential energy due to electronic excitation.

The fast atomic motion in a fast excited solid can also be qualitatively described using the interatomic interaction potential (Morse potential) shown in **Figure 7**. In fact, the interatomic potential is composed of the part that attracts electrons and the part that repels ion nuclei. Fast electron excitation reduces the attraction and therefore the binding energy. The distance between atoms increases due to the excitation of electrons. Compared with the quantum harmonic oscillator model potential, the interatomic potential in Morse contains the nonbonded state that is absent from the harmonic oscillator model, so it can describe the nonharmonic effect, frequency doubling, and combination frequency [58]. Morse potential expresses the atomic displacement as a function of electron temperature, binding energy, equilibrium atomic spacing, and the gradient of attraction and repulsion of the potential.

Based on the consideration of the above model potential, analyze the atomic vibration in an undisturbed solid, consider first-order approximation, ignore spatial dispersion, and consider the excited phonon as a standing wave. The elastic force driving harmonic vibrations in solids can be represented by the second-order perturbation term in the interatomic potential, which is in the form of:

$$\Delta U_{el} = \frac{1}{2}\left(\frac{\partial^2 U}{\partial q^2}\right)_0 q^2 \approx \frac{1}{2} M\omega_0^2 q^2 \tag{4}$$

One estimates $\left(\partial^2 U/\partial q^2\right)_0 \approx \varepsilon_b/d^2$; here q is the cold phonon amplitude, ε_b is the binding(cohesive) energy, and d is the interatomic distance in equilibrium. The cold phonon frequency in Eq. (4) is $\omega_0^2 \approx \varepsilon_b/Md^2$. The elastic force driving harmonic vibrations immediately follows from Eq. (4):

$$F_{el} = \frac{\partial \Delta U_{el}}{\partial q} \approx M\omega_0^2 q \tag{5}$$

The cold phonon amplitude at a temperature lower than the Debye temperature is estimated as [59]:

$$q_0 \approx \left(\frac{2\hbar}{M\omega_0}\right)^{1/2} \tag{6}$$

Now, the elastic force explicitly expresses through the basic characteristics of a solid:

$$F_{el} \approx \left(M\omega_0^3\hbar\right)^{1/2} \tag{7}$$

Considering the effect of a laser electric field on the material under constant volume conditions, the laser causes internal atomic motion that leads to material deformation, thereby modulating the dielectric function of the medium. The stress tensor of the initial isotropic medium can be expressed as [60]:

$$\sigma_{ik} = -P\delta_{ik} - \left(\frac{E^2\delta_{ij}}{8\pi} + \frac{E_iE_j}{4\pi}\right)\varepsilon_{jk} + \frac{E^2}{8\pi}\left[n_a\left(\frac{\delta\varepsilon_{jk}}{\delta n_a}\right)_T\right]\delta_{ij} + \frac{E_iD_k}{4\pi}, \tag{8}$$

where the electric displacement vector has a form $D_k = \varepsilon_{kj}E_j$. We assume that the dielectric tensor modified by the laser effect consists of two terms, the Drude-like term, ε_D, and polarization term, $\varepsilon_{jk}^{(p)}$:

$$\varepsilon_{jk} = \varepsilon_D\delta_{jk} + \varepsilon_{jk}^{(p)} \tag{9}$$

The electron number density, dielectric function, electron and lattice temperature in transient are all time-dependent.

The volume force caused by the laser field can be represented by the stress tensor modulated by the field effect, σ_{ik}, taken from Eq. (8) as follows [61]:

The volume force caused by the laser field is expressed by the stress tensor σ_{ik} modified by the field action, which is taken from Eq. (8) as follows [61]:

$$f_i = \frac{\delta\sigma_{ik}}{\delta x_k} = -\frac{\delta P}{\delta x_k} + \frac{\delta\varepsilon_{ik}^{(p)}}{\delta x_k}\frac{E^2}{8\pi} + \frac{(\varepsilon_D - 1)}{8\pi}\frac{\partial E^2}{\partial x_i} = f_i^{th} + f_i^{(p)} + f_i^{pond} \tag{10}$$

Here, we consider that for the Druid-like part of the dielectric function, the following relation holds, $n_a(\partial\varepsilon_D/\partial n_a)T = \varepsilon_D - 1$. The first term on the right side of Eq. (10) is the thermal driving force caused by the above electron temperature gradient. The second term is the force related to polarization, based on the Plazcek effect [62], whose magnitude is inversely proportional to the atomic displacement, and the third term is the ponderomotive force. Polarization and ponderomotive force are only effective during the duration of the pulse, while thermal driving forces cause atomic movement until the temperature gradient is smooth throughout space. It is also worth noting that the polarization force in Eq. (10) is similar to but different from the force driving phonon excitation in the Raman effect [63]. This difference is related to the fact that the duration of the laser pulse is much shorter than the phonon period. Therefore, there is no interaction between the laser electric field and the vibration field of atomic motion. The phonon frequency enters the polarization force indefinitely.

The spatial variation based on optical power density forms the ponderomotive force acting on atoms or electrons or ions in the dielectric or plasma. The optical

power density of a monochromatic plane wave is independent of distance, and the longitudinal component of ponderomotive force is zero. For traveling pulses in dispersive media, their spatial range varies with the variation of optical group velocity. At small group velocities, moderate pulse energy also transfers a large amount of momentum to the atoms colliding with it. The strong excitation of lattice atoms with large momentum at once leads to ionization, desorption, and ablation, which presents typical nonlinear characteristics.

Based on the above qualitative discussion about the structural relaxation of materials after pulse laser action. Briefly explain the ultrashort interaction mode, that is, the duration of the laser pulse is far less than the time of the energy equilibration in the irradiated material. Obviously, nonequilibrium phenomena dominate the material removal mode, one of which is the rapid formation of lattice distribution functions with truncated high-energy tails, which can lead to different ablation modes.

6. Conclusion

To sum up, this chapter first analyzes the interaction between laser and matter from the perspective of energy, describes the electronic response characteristics of semiconductors and insulating dielectric materials excited by nanosecond pulse laser and femtosecond pulse laser, explores the relaxation process of the interaction between excited electrons and lattice, and analyzes the generation mechanism of polarization force and pondermotive force acting on lattice based on the multiple coupling of laser field and plasma. At the same time, the basic analysis of the above laser-matter interaction process is given based on molecular dynamics. These effects may modulate the relevant physical processes of ionization, desorption, and ablation. It is hoped that the theoretical analysis results of the interaction between laser and materials in this chapter will have certain guiding significance for the related fields of laser processing, laser spectral analysis, and process design of periodic surface structure beyond the optical diffraction limit.

Author details

Hong Liu* and Chunlan Ma
School of Physical Science and Technology, Suzhou University of Science and Technology, Suzhou, China

*Address all correspondence to: hliu@usts.edu.cn

References

[1] Pariz I, Goel S, Nguyen DT, Buckeridge J, Zhou X. A critical review of the developments in molecular dynamics simulations to study femtosecond laser ablation. Materials Today: Proceedings. 2022;**64**: 1339-1348

[2] von Allmen M. Laser-beam interactions with materials. In: Springer Ser. Mater. Sci. Vol. 2. Berlin, Heidelberg: Springer; 1987

[3] Orazi L, Romoli L, Schmidt M, Li L. Ultrafast laser manufacturing: From physics to industrial applications. CIRP Annals - Manufacturing Technology. 2021;**70**:543-566

[4] Harilal S et al. Optical spectroscopy of laser produced plasmas for standard isotopic analysis. Applied Physics Reviews. 2018;**5**(2):021301

[5] Bogaerts A, Chen Z. Effect of laser parameters on laser ablation and laser-induced plasma formation: A numerical modeling investigation. Spectrochimica Acta Part B: Atomic Spectroscopy. 2005; **60**(9–10):1280-1307

[6] Bogaerts A et al. Laser ablation for analytical sampling: What can we learn from modeling? Spectrochimica Acta Part B: Atomic Spectroscopy. 2003;**58** (11):1867-1893

[7] Boueri M et al. Early stage expansion and time-resolved spectral emission of laser-induced plasma from polymer. Applied Surface Science. 2009;**255**(24): 9566-9571

[8] Yoo JH et al. Existence of phase explosion during laser ablation and its effects on inductively coupled plasma-mass spectroscopy. Analytical Chemistry. 2001;**73**(10):2288-2293

[9] Chen Z, Bogaerts A. Laser ablation of cu and plume expansion into 1 atm ambient gas. Journal of Applied Physics. 2005;**97**(6):063305

[10] Bogaerts A, Chen Z. Nanosecond laser ablation of cu: Modeling of the expansion in He background gas, and comparison with expansion in vacuum. Journal of Analytical Atomic Spectrometry. 2004;**19**(9):1169-1176

[11] Bonse J, Höhm S, Kirner SV, Rosenfeld A, Krüger J. Laser-induced periodic surface structures— A scientific evergreen. IEEE Journal of Selected Topics in Quantum Electronics. 2017; **23**(3):9000615

[12] Link S, El-Sayed MA. Optical properties and ultrafast dynamics of metallic nanocrystals. Annual Review of Physical Chemistry. 2003;**54**(1):331-366

[13] Hu M et al. Gold nanostructures: Engineering their plasmonic properties for biomedical applications. Chemical Society Reviews. 2006;**35**(11):1084-1094

[14] Zhang JZ, Noguez C. Plasmonic optical properties and applications of metal nanostructures. Plasmonics. 2008; **3**(4):127-150

[15] Wang L, Hasanzadeh Kafshgari M, Meunier M. Optical properties and applications of Plasmonic-metal nanoparticles. Advanced Functional Materials. 2020;**30**(51):2005400

[16] Linic S, Christopher P, Ingram DB. Plasmonic-metal nanostructures for efficient conversion of solar to chemical energy. Nature Materials. 2011;**10**(12): 911-921

[17] Taliercio T, Biagioni P. Semiconductor infrared plasmonics. Nanophotonics. 2019;**8**(6):949-990

[18] Henry H. Laser Precision Microfabrication. In: Sugioka K, Meunier M, Piqué A, editors. Berlin, Heidelberg: Springer; 2010. ISBN: 978-3-642-10522-7

[19] Soltani B, Azarhoushang B, Zahedi A. Laser ablation mechanism of silicon nitride with nanosecond and picosecond lasers. Optics and Laser Technology. 2019;**119**:105644

[20] Jandeleit J, Horn A, Weichenhain R, Kreutz EW, Poprawe R. Fundamental investigations of micromachining by nano- and picosecond laser radiation. Applied Surface Science. 1998;**127–129**: 885-891. DOI: 10.1016/S0169-4332(97) 00762-9

[21] Tuennermann A, Nolte S, Limpert J. Femtosecond vs picosecond laser material processing. Laser Technik Journal. 2010;7(1):34-38. DOI: 10.1002/ latj.201090006

[22] Kumar M, Melkote S, Lahoti G. Laser-assisted microgrinding of ceramics. CIRP Annals - Manufacturing Technology. 2011;**60**(1):367-370. DOI: 10.1016/j.cirp. 2011.03.121

[23] Vogel A, Venugopalan V. Mechanisms of pulsed laser ablation of biological tissues. Chemical Reviews. 2003;**103**(2):577-644. DOI: 10.1021/ cr010379n

[24] von der Linde D, Sokolowski-Tinten K. The physical mechanisms of short-pulse laser ablation. Applied Surface Science. 2000;**154–155**:1-10. DOI: 10.1016/S0169-4332(99)00440-7

[25] Kienberger E, Goulielmakis M, Uiberacker A, Baltuska V, Yakovlev F, Bammer A, et al. Atomic transient recorder. Nature. 2004;**427**(33): 817-821

[26] Steen WM, Mazumdar J. Laser Material Processing. Springer Verlag, fourth ed. 2010. ISBN 978-1-84996-061-8

[27] Li X, Guan Y. Theoretical fundamentals of short pulse laser–metal interaction: A review. Nanotechnology and Precision Engineering. 2020;**3**:105-125

[28] Rethfeld B et al. Modelling ultrafast laser ablation. Journal of Physics D: Applied Physics. 2017;**50**(19):193001

[29] Sundaram S, Mazur E. Inducing and probing non-thermal transitions in semiconductors using femtosecond laser pulses[J]. Nature Materials. 2002;**1**(4): 217-224. DOI: 10.1038/nmat767

[30] Yang G. Laser Ablation in Liquids: Principles and Applications in the Preparation of Nanomaterials. CRC Press; 2012. DOI: 10.1201/b11623. ISBN: 9780429086106

[31] Stolee JA et al. Laser–nanostructure interactions for ion production. Physical Chemistry Chemical Physics. 2012;**14** (24):8453-8471

[32] Joshi A, Majumdar A. Transient ballistic and diffusive phonon heat transport in thin films. Journal of Applied Physics. 1993;**74**(1):31-39

[33] Singh AP, Kapoor A, Tripathi KN. Ripples and grain formation in GaAs surfaces exposed to ultrashort laser pulses. Optics and Laser Technology. 2002;**34**:533-540

[34] Singh AP, Gaur SS. Attosecond laser-matter interaction: A short note. Materials Today: Proceedings. 2022;**64**: 295-297

[35] Maiuri M, Garavelli M, Cerullo G. Ultrafast Spectroscopy: State of the Art and Open Challenges. Journal of the

American Chemical Society. 2020; **142**:3-15

[36] Lazic V, Jovićević S. Laser induced breakdown spectroscopy inside liquids: Processes and analytical aspects. Spectrochimica Acta Part B: Atomic Spectroscopy. 2014;**101**: 288-311

[37] Dharmadhikari J et al. Optical control of filamentation-induced damage to DNA by intense, ultrashort, near-infrared laser pulses. Scientific Reports. 2016;**6**(1):1-9

[38] Linz N et al. Wavelength dependence of femtosecond laser-induced breakdown in water and implications for laser surgery. Physical Review B. 2016;**94**(2):024113

[39] Vanraes P, Bogaerts A. Plasma physics of liquids - a focused review. Applied Physics Reviews. 2018;**5**(3): 031103

[40] Balling P, Schou J. Femtosecond-laser ablation dynamics of dielectrics: Basics and applications for thin films. Reports on Progress in Physics. 2013;**76** (3):036502

[41] Du D, Liu X, Korn G, Squier J, Mourou G. Laser induced breakdown by impact ionization in SiO_2 with pulse widths from 7 ns to 150 fs. Applied Physics Letters. 1994;**64**:3071-3073

[42] Stuart BC, Feit MD, Herman S, Rubenchik AM, Shore BW, Perry MD. Optical ablation by high-power short-pulse lasers. Journal of the Optical Society of America B. 1996;**13**: 459-468

[43] Kruer WL. The Physics of Laser Plasma Interactions. New-York: Addison-Wesley Publishing; 1988

[44] Gamaly EG, Rode AV, Luther-Davies B, Tikhonchuk VT. Ablation of solids by femtosecond lasers: Ablation mechanism and ablation thresholds for metals and dielectrics. Physics of Plasmas. 2002;**9**:949-957

[45] Kramer T et al. Ablation dynamics–from absorption to heat accumulation/ ultra-fast laser matter interaction. Advanced Optical Technologies. 2018; **7**(3):129-144

[46] Zhigilei LV, Lin Z, Ivanov DS. Atomistic modeling of short pulse laser ablation of metals: Connections between melting, spallation, and phase explosion. Journal of Physical Chemistry C. 2009; **113**(27):11892-11906

[47] Chichkov BN et al. Femtosecond, picosecond and nanosecond laser ablation of solids. Applied Physics A. 1996;**63**(2):109-115

[48] Yilbas B et al. Laser-shock processing of steel. Journal of Materials Processing Technology. 2003;**135**(1):6-17

[49] Zeng X et al. Experimental investigation of ablation efficiency and plasma expansion during femtosecond and nanosecond laser ablation of silicon. Applied Physics A. 2005;**80**(2):237-241

[50] Liu C et al. Nanosecond and femtosecond laser ablation of brass: Particulate and ICPMS measurements. Analytical Chemistry. 2004;**76**(2): 379-383

[51] Lu Q et al. Delayed phase explosion during high-power nanosecond laser ablation of silicon. Applied Physics Letters. 2002;**80**(17):3072-3074

[52] Lu Q et al. Theory analysis of wavelength dependence of laser-induced phase explosion of silicon. Journal of Applied Physics. 2008;**104**(8):083301

[53] Russo RE et al. Femtosecond laser ablation ICP-MS. Journal of Analytical Atomic Spectrometry. 2002;**17**(9): 1072-1075

[54] Lee Y et al. Spatial and temporal distribution of metal atoms and their diatomic oxide molecules in femtosecond laser-induced plasmas. Journal of Analytical Atomic Spectrometry. 2018;**33**(11): 1875-1883

[55] Ionin AA, Kudryashov SI, Samokhin AA. Material surface ablation produced by ultrashort laser pulses. Physics-Uspekhi. 2017;**60**(2):149

[56] Gamaly EG, Rode AV. Physics of ultra-short laser interaction with matter: From phonon excitation to ultimate transformations. Progress in Quantum Electronics. 2013;**37**(5):215-323

[57] Klett I, Rethfeld B. Relaxation of a nonequilibrium phonon distribution induced by femtosecond laser irradiation. Physical Review B. 2018;**98** (14):144306

[58] Morse PM. Diatomic molecules according to the wave mechanics. II. Vibrational levels. Physical Review. 1929;**34**:57

[59] Il'inskii YA, Keldysh LV. Electromagnetic Response of Material Media. New York: Springer; 1994

[60] Landau LD, Lifshitz EM, Pitaevskii LP. Electrodynamics of Continuous Media. Oxford: Pergamon Press; 1984

[61] Kent AJ, Kini RN, Stanton NM, Henini M, Glavin BA, Kochelap VA, et al. Acoustic phonon emission from a weakly coupled superlattice under vertical electron transport: Observation of phonon resonance. Physical Review Letters. 2006;**96**:215504

[62] Gamaly EG. The physics of ultra-short laser interaction with solids at non-relativistic intensities. Physics Reports. 2011;**508**:91-243. DOI: 10.1016/j.physrep.2011.07.002

[63] Shen YR, Bloembergen N. Theory of stimulated Brillouin and Raman scattering. Physical Review. 1965;**137**: 1787-1805